# Energy Dispersive X-ray Reflectometry of the $NO_2$ Interaction with Ruthenium Phthalocyanine Films

**Amanda Generosi,[†,‡] Valerio Rossi Albertini,[†] Gentilina Rossi,[§] Giovanna Pennesi,[§] and Ruggero Caminiti*[,§]**

*Istituto di Struttura della Materia (CNR), Via del Fosso del Cavaliere 100, 00133 Roma, Italy, Istituto di Struttura della Materia (CNR), Via Salaria Km.29.5, CP10 Monterotondo Stazione, Roma, Italy, and Dipartimento di Chimica, Istituto Nazionale per la Fisica della Materia, Università di Roma "La Sapienza", P.le Aldo Moro 5, Roma, Italy*

*Received: August 7, 2002; In Final Form: October 17, 2002*

The X-ray reflectrometry technique in its energy dispersive variant (EDXR) is utilized to study the morphological characteristics of dimeric ruthenium phthalocyanine $(RuPc)_2$ thin films, which are being exploited as nitrogen oxide gas sensors. The advantages of the EDXR with respect to its conventional (angular dispersive) counterpart are discussed. The high sensitivity of this technique allowed us to detect minimal variations of the films thickness and roughness as a consequence of the exposure to a $NO_2$ gas flux, providing information on the gas diffusion process through the film and on the mechanisms of interaction between film and gas molecules.

## Introduction

Phthalocyanines (Pcs) and metallophthalocyanines (Mpcs) have been investigated in detail for many years because of their properties as dyestuffs, paints, and colors.[1] In the past decades phthalocyanine chemistry has undergone a renaissance because these compounds and their derivatives exhibit semiconducting or conducting properties of technological interest for electronic devices.[2] Phthalocyanines can present several kinds of condensed phases: single crystalline, amorphous Langmuir−Blodget films and liquid crystals. Thanks to this versatility, phthalocyanine compounds can be organized to achieve supramolecular properties and can be easily incorporated in molecular devices. Because in most of the molecular and macromolecular phthalocyanine systems the difference between the oxidation and reduction potentials is equal to or greater than 1.5 eV, the radical phthalocyanines may therefore be used as molecular semiconductors.[3] It is also well-known that the electrical properties of the phthalocyanines (Pcs) are modulated upon exposure to gases such as $NO_2$ or ammonia, opening a promising route in developing gas detectors using Pc derivatives as the chemically sensitive component.[4]

The gas adsorption/desorption processes of MPcs films depend mainly on the material's redox potential, but surface morphology and molecular arrangement play a relevant role as well as affecting both charge transfer interaction and charge carrier transport. We know that gas sensing features, such as response time, reproducibility, and reversibility, can be improved by knowledge of the physical−chemical phenomena that occur at the gas−material interface. Because these interactions are not fully understood, important information gained by investigating the changes occurring in Mpcs thin films upon gas exposure, i.e., thickness and roughness variations, may contribute to improvement in sensor feature.

For this purpose we used X-ray reflectometry in the energy dispersive mode, a technique sensitive to surface and interface morphology at the angstrom resolution to obtain information on the interaction process between RuPc films and $NO_2$ gas because this system is at present the object of an extensive study for its potential application as an optical/conductometric sensor.

## Experimental Section

**Theory.** The X-ray reflectometry method makes use of the optical properties of X-rays.

From Snell law of classic optics, when a light beam passes through the interface between two media having different refractive indexes, it is deviated from its original direction. In particular, if the index of the second medium is lower, the beam will be totally reflected when the incident angle is below a threshold (critical angle $\theta_c$). In optics, the refractive index is an increasing function of the density, so that the total reflection occurs by passing from the more to the less dense medium (for instance from condensed matter to air). Snell rule still applies in the X-ray energy range. However, the relationship between density and refractive index is inverted, so that the total reflection is observable passing from a less to a more dense material (from air to condensed matter). This fact enables one to use the reflectometry as a tool for physical and material science studies because an X-ray beam impinging a sample (either in air or in a vacuum) can be totally reflected by it, carrying morphological information on the reflection surface.

Measuring the incidence and reflection angles from the surface (instead of from the normal to it), Snell law can be written as $n_1 \cos \theta_1 = n_2 \cos \theta_2$. If $n_1 > n_2$, then $\theta_1 > \theta_2$ and there must be a value of $\theta_1$, called the *critical angle* $\theta_c$, so that, for a sample in air $\cos \theta_c = n_2$ because $\theta_2 = 0$. In these conditions the beam will not be refracted any more, but totally reflected.

* Corresponding author. Fax: +36-06-490631. E-mail: r.caminiti@caspur.it.

† Istituto di Struttura della Materia (CNR), Via del Fosso del Cavaliere 100.

‡ Istituto Nazionale per la Fisica della Materia.

§ Istituto di Struttura della Materia (CNR), Via Salaria Km.29.5.

10.1021/jp021846n CCC: $25.00 
Published on Web 12/18/2002

In the case of X-rays the real part of $n$ is slightly less than 1. In fact, the general expression of the complex refractive index for X-rays is

$$n = 1 - (\lambda^2/2\pi)\rho r_0 Z^2 + i(\lambda/4\pi)\mu$$

where $\lambda$ is the incident wavelength, $\rho$ is the material density, $r_0$ is the classical electron radius, $Z$ is the atomic number, and $\mu$ is the linear absorption coefficient. The imaginary component is responsible for the absorption and will be neglected because the beam in total reflection conditions penetrates only a thin layer of the material[5] and its value is generally $10^{-6}-10^{-7}$. Starting from this expression, we can rewrite Snell law for an incident X-ray beam, substituting the expression of $n$ into the equation: $\cos\theta_c = n_2$, obtaining: $\cos\theta_c = 1 - \rho\lambda^2 r_0 Z^2/2\pi$.

Because the values of $\theta_c$ are very small, this expression can be developed in McLauren powers around $\theta = 0$, $1 - \theta_c^2/2 = 1 - \rho\lambda^2 r_0 Z^2/2\pi$, thus finally deducing that $(\theta_c/\lambda) = Z(\rho r_0/2)^{1/2} =$ constant is a different way to express the Snell law for X-rays upon total reflection.

Moreover, at the second-order approximation, $\theta_c/\lambda \approx \sin\theta/\lambda \propto q$. Therefore in a total reflection experiment, the relevant parameter is not the critical angle alone, because it is defined only when the radiation wavelength is selected: changing the wavelength also changes the critical angle. What does not vary is the ratio, which is a quantity proportional to the momentum transfer: $q = 4\pi \sin\vartheta/\lambda = (2/hc)E \sin\vartheta$. To collect information in a certain range of $q$, two different possibilities are available, either working with a fixed wavelength and performing an angular scan (ADXR) or maintaining a fixed angular position and using a range of energies to make the scan (EDXR). When an X-ray reflectivity experiment is performed, the advantages of this technique are remarkable, and the disadvantages become irrelevant. In fact, the immobility of the apparatus during data collection becomes fundamental because, unlike ADXR, no movement is required, which simplifies the experimental procedure and prevents systematic errors. But the most important feature is related to the resolution in the $q$ space. A single spectrum collected at fixed angle, using the whole white beam produced by a conventional W-anode source, covers typically a range of some $10^{-2}$ Å$^{-1}$. In this range we collect a few hundred points whose number is reduced by a factor 5, because groups of 5 adjacent points are summed to take into account the energy resolution of the SSD. To get the same resolution using a $k_\alpha$ of Cu as primary beam, in the same $q$ range, angular steps of some 0.001° are required. Further advantages are the increase of the signal intensity and the parallel collection of the spectra.[6]

On the other hand, the main drawback connected to the energy dispersive mode, i.e., the decrease in $q$ resolution because of the joint uncertainties on both the angle and the energy, becomes irrelevant in reflectometry experiments. In fact, total reflection spectra are characterized by broad peaks or oscillations that are not remarkably affected by a further slight broadening.

As mentioned above, a more proper way to describe the reflectivity spectra is to express the reflected intensity as a function of the scattering parameter $q$. When $q < q_c$, the X-ray radiation impinging on the sample is totally reflected, that is the incident and reflected beams have the same intensity and the reflectivity $= I_{reflected}/I_{incident} = 1$. When $q \approx q_c$, the radiation starts penetrating the sample, and as soon as $q > q_c$, the reflectivity decays more than exponentially. In this threshold profile is the region of interest in X-ray reflectivity measurement, as the information about the surface is contained in it.

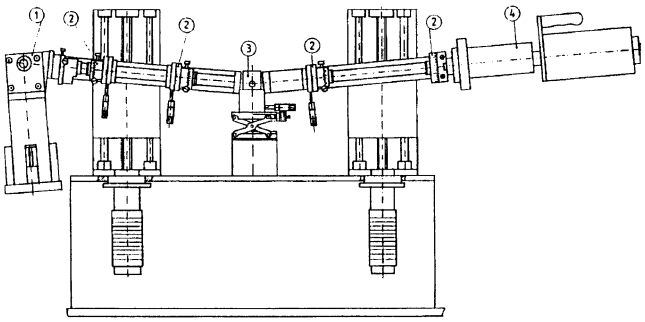

**Figure 1.** Schemathic drawing of the energy-dispersive X-ray noncommercial reflectometer, Istituto Struttura della Materia, CNR, Roma, Italy: (1) X-ray tube; (2) collimation slits; (3) sample position; (4) single cristal solid state energy sensitive detector.

The reflectivity profile of an X-ray beam impinging the sample surface (air−sample interface), as a function of $q$, contains information about the irradiated surface material. Indeed, the position of the critical edge ($q = q_c$) and the inclination of the threshold are determined by the material density and the surface roughness (defined as the variance from the average thickness), respectively. To understand how information on a film can be gained by reflectivity measurements, a simplified model can be used. When the X-ray beam impinges two stratified media, it is partially reflected at two interfaces: air/medium$_1$ and medium$_1$/medium$_2$, the two reflected beams will interfere, producing an almost sinusoidal modulation of the reflectivity. The period of the modulation is proportional to the inverse of the distance between the two interfaces, i.e., to the film thickness, whereas the inclination of the threshold and the damping of the oscillations are related to both the surface and the interface roughness. However, to fit the experimental data, a more realistic model[7] will be used.

**EDXR Apparatus.** An energy-dispersive X-ray reflectometer,[8,9] Figure 1, differs from an angular dispersive apparatus, because of the absence of a monocromathor and goniometer. The instrument is mechanically very simple, with two arms contained in the vertical plane, pivoting around a single central axis. The arms are moved by two linear actuators driven by step motors and the tangent of the angles of inclination is read by two linear encoders. Both the minimum step movement and the resolution of the encoders are 1 $\mu$m, leading to a minimum angle increment and reproducibility of 0.0004°. The X-ray optical path is defined by four variable slits (2 mm W) mounted on the arms. The source is a standard 2 kW tungsten anode X-ray tube, producing a white beam whose useful energy range is from 12 (above the last L fluorescence line of W) to 58 keV. Because the $q$ range covered in a single measurement is usually not large enough to observe a number of oscillations sufficient to perform a good fit of the reflectivity curve, several runs at various angles are necessary. Indeed, by increasing the measurement angle, zone of the reciprocal space corresponding to progressively higher $q$ values are scanned. The various pieces of the reflectivity curve are then united, utilizing the partial overlap of adjacent zones. The scale factor is calculated by integration of these overlap regions. In this way, a uniquely wide $q$ curve is obtained.

The X-ray detection is accomplished by an EG&G high-purity germanium solid-state detector connected via ADCAM hardware to a personal computer running the Maestro software to visualize and record the data through a multichannel analyzer. The energy resolution is ca. 1.5% with a maximum count rate of 10 kcounts/s.

The measurement of the incident spectra is necessary to normalize the reflectivity data. It is acquired by placing the two arms in straight position (0° inclination angle**),** and collecting the direct beam spectrum.

**Films Deposition and Exposure to Gas.** The ruthenium phthalocyanine thin films were obtained by sublimation under vacuum of RuPc powder[10] according to the procedures previously reported.[11] An Edwards Auto 306 vacuum coater with diffusion pumping system, capable of reaching $10^{-5}-10^{-6}$ mbar of pressure, has been used to prepare the films on substrates of a Si ⟨111⟩ wafer. The growth was observed by an Edwards FTM5 film thickness monitor, measuring the change in the resonance frequency of a quartz crystal[12] due to its mass increase accompanying film deposition .

Various films having nominal thickness in the range 200−1500 Å were grown.

The films after a first EDXR investigation were exposed to 100 ppm of $NO_2$ in air (flow = 500 sccm) for a couple of hours; the gas interaction leads to a charge-transfer complex with a defined optical spectrum.[13] Visible spectra registered during the process allow us to follow the reaction that we considered complete when spectral changes were not observed any more. The presence in the visible spectrum of a clear isosbestic point demonstrated that the transition to the new oxidized complex was quantitative and no intermediate species were produced during the interaction process.

A computer aided apparatus with a Keithley 236 source measuring unit connected to the electrode was used for recording current as function of time. All experiments were carried out at room temperature.

At this step the films were again analyzed by the EDXR technique and the changes in their morphology were monitored.

## Results and Discussion

We have recently reported[11] the structural characterization of ruthenium phthalocyanines films using energy dispersive X-ray diffraction, proving this technique is a promising tool for structural investigation of an amorphous film. These diffraction data indicated that, in the passage from the bulk to the film, the dimeric structure of the compound was maintained, the only change being the different length of columnar packing of dimeric molecules, more wide ranging in the film than in the bulk material; indeed, 10 dimers were superimposed along the stacking direction (parallel to the Ru−Ru bonds), whereas six units were found in the bulk material. The higher order observed was also supported by conductivity measurements. The arrangement in a one-dimensional stacking of this compound is responsible for the electrical properties ($\sigma = 1 \times 10^{-4}\ \Omega^{-1}\ cm^{-1}$), but a relevant role of the metal surely underlines the strong reactivity showed toward small molecules like $NO_2$. For these peculiarities the compound appeared worthy of investigation as a chemical sensor. In another study we found that the UV−visible spectra registered during the interaction of the compound with $NO_2$, clearly indicated the formation of a new species with characteristic spectral features.[13] However, the reaction mechanism, the role of metal, and of the macrocycle in the oxidation process is not completely defined. Therefore, to improve the reversibility and to shorten the response time of the sensor, it is necessary to understand if the process involves the whole bulk or the surface only. For this reason, to gain useful information, the present EDXR study was performed on the material before and after gas adsorption, starting with the determination of the films real thickness.

The thickness and roughness were calculated from the collected data, using the Parrat model. In physics textbooks it is affirmed that systems characterized by certain distances can be studied using probes having a wavelength of the same order of magnitude of such distances: the modalities with which the probe is scattered provide the required information on the distances. However, considering the Bragg equation, $2d \sin\theta = n\lambda$, it can be noticed that the comparison should be rather done between the probe wavelength and the product of the distance by the (sine of) the scattering angle. Therefore, by reducing this angle, a probe having a certain $\lambda$ can be utilized to investigate a sample with much larger characteristic distances. This applies both to small angle scattering and to X-ray reflectivity measurements. X-rays with wavelengths shorter than 1 Å can investigate film thicknesses up to several thousands of ångstroms (dependent on the optical contrast with the substrate).

The Parrat model describes the intensity of a radiation reflected by a thin film and separated from the substrate, on which it is deposited, by a sharp interface:

$$|R|^2 = \{1 - 2[\mathrm{Re}(R_l R_r - R_l R_r)\exp(-2kd)]/ [1 + \exp(-4kd) - 2\mathrm{Re}(R_l R_r)\exp(-2kd)]\} \quad (1)$$

where $k_0 = q/2$ is the radiation wavenumber in the air, $R_l = (k_0 - k_f)/(k_0 + k_f)$ is the Fresnel film material reflectivity, $R_r = (k_f - k_s)/(k_f + k_s)$ is the Fresnel substrate material reflectivity, and $d$ is the film average thickness. The quantities $k_f$ and $k_s$ are the radiation wavenumbers in the film and in the substrate, which depend strongly on $k_0$: $k_f = (k_0^2 - 4\pi\rho_f)^{1/2}$ and $k_s = (k_0^2 - 4\pi\rho_s)^{1/2}$.

When the surface or the interface is not sharp, the reflected intensity is modified by a roughness term similar to a Debye−Waller factor.[14] In our case, because the substrate is monocrystal, the roughness of the interface is much smaller than that of the surface and will be neglected.

Considering surface roughness only, the general expression for the reflected intensity become

$$|R|^2 = \{|R_l|^2\exp(-2k_0k_f\sigma^2)| + |R_r|^2 - 2\mathrm{Re}[R_lR_r\exp(-2k_0k_f\sigma^2)\exp(2ik_fd)]/ 1 + |R_l|^2|R_r|^2\exp(-2k_0k_f\sigma^2)| - 2\mathrm{Re}[R_lR_r\exp(-2k_0k_f\sigma^2)\exp(2ik_fd)]\} \quad (2)$$

The data were fitted according to the theoretical model discussed above. Five free parameters were used in the fit, one to normalize the intensities due to different counting times, the others to obtain morphological information, i.e., film average thickness and roughness. In Figure 2, the reflectivity profiles of the five samples are shown in semilog graphs, together with their fits. The corresponding numerical results of thickness and roughness are reported in Table 1. The two samples (400 and 1000 Å) showing the best reflectivity profiles were exposed to $NO_2$ gas and measured again. The oscillating components of the curves above their critical $q$ value were extracted by normalizing the collected spectra according to eq 2. In Figure 3, such components for the 400 Å thick sample, before and after the exposure to gas, are plotted. The oscillations appear to progressively get out of phase, revealing a variation in the film thickness, and to have a different damping, which can be attributed to the increase of the surface roughness. In Figure 4, the same behavior is observed in the case of the 1000 Å thick sample.

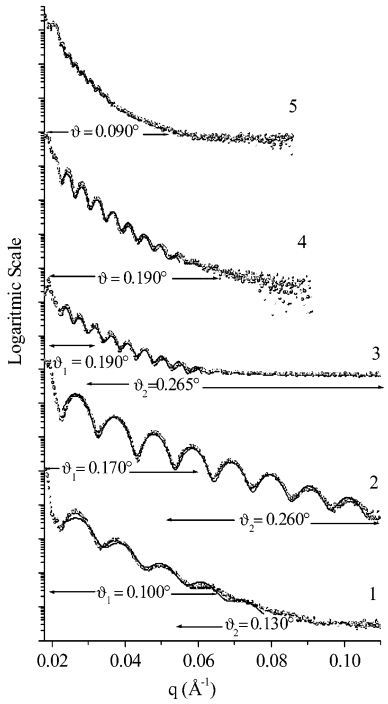


**Figure 2.** Total reflection measurements of ruthenium phthalocyanine thin films (dotted line) and calculated data (solid line) versus (1) 200 Å nominally thick film, (2) 400 Å nominally thick film, (3) 750 Å nominally thick film, (4) 1000 Å nominally thick film, and (5) 1500 Å nominally thick film.

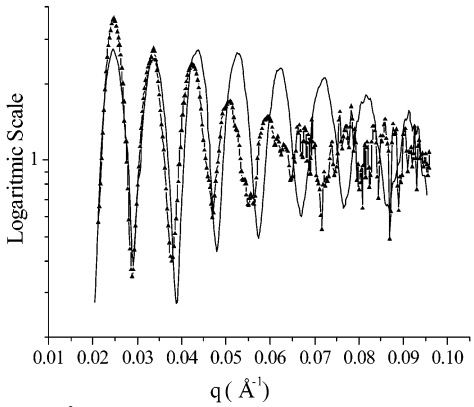


**Figure 3.** 400 Å thick RuPh film signal only, before (solid line) and after (dotted line) interaction with $NO_x$. Changes in frequency and amplitude are visible due to the solid/vapor interaction.

**TABLE 1: Thickness (Å) and Roughness (Å) of the RuPh Films Calculated from the Experimental Data, versus the Nominal Values Obtained during the Deposition**

| nominal thickness | measured thickness | roughness |
|---|---|---|
| 200 | 254.5 | 8.2 |
| 400 | 328.3 | 6.4 |
| 750 | 658 | 9.4 |
| 1000 | 732.3 | 14.3 |
| 1500 | 1949.3 | 24 |

In Table 2, the comparison between the values of thickness and roughness before and after exposure to $NO_x$ are reported.

From Figures 3 and 4 some interesting information can be deduced on how the gas interacts with the film, discarding interpretations of the process that are not consistent with experimental evidences. Indeed, the high sensitivity of this technique to the morphological characteristics of thin films coupled with the high accuracy of the measurement provides some important indications with which the whole interaction phenomenon has to be necessarily in agreement.

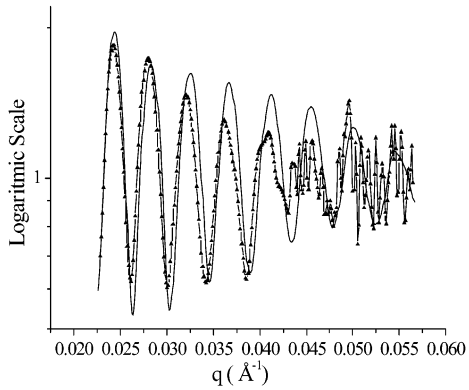


**Figure 4.** 1000 Å thick RuPh film signal only, before (solid line) and after (dotted line) interaction with $NO_x$. Changes in frequency and amplitude are visible due to the solid/vapor interaction.

**TABLE 2: Thickness (Å) and Roughness (Å) of Two RuPh Films (400 and 1000 Å Respectively), before and after $NO_x$ Exposure**

| RuPh films | 400 Å nominally | 1000 Å nominally |
|---|---|---|
| thickness before exposure | 328.3 | 732.3 |
| thickness after exposure | 355 | 745 |
| roughness before exposure | 6.4 | 14.33 |
| roughness after exposure | 15.5 | 18.8 |

The interaction does not appear to be restricted to the surface of the film and, therefore, with the model of absorption (or chemisorption) of a gas molecule layer. If so, the increase in the thickness of the two samples should be comparable, whereas it appears to be quite different in the two samples (see Table 2). This result has been supported also by XPS depth profile registered on the same RuPc films.[15] However, from the obtained EDXR data it appears that the interaction is not uniform in the bulk; otherwise, the thickness increase should be proportional to its initial value. Instead, the experimental results show that the increase is higher in the thinner film than in the thicker one (Table 2). The same trend is observed for the roughness variation as a consequence of the exposure to the gas, the increase being more pronounced in the 400 Å film than in the 1000 Å one.

These results can find a reasonable answer considering the strong molecular rearrangement expected for this dimeric system as chemical transformation to a monomeric species with more disordered packing, both tending to minimize the volume increase produced by gas interaction.

## Conclusions

The application of energy dispersive X-ray reflectometry consented a detailed study of thin films of Ru−phthalocyanine thin films and of their morphological change as a consequence to the exposure to $NO_x$ gas flux.

The measurements provide evidence to reject chemical models based on surface interaction or on uniform diffusion of gas molecules inside the bulk because the thickness increments due to gas exposure are neither constant nor proportional to the initial thickness of the film. New experiments to follow the gas-film interaction "in situ" by time-resolved total reflection measurements are in progress to obtain information on the chemical mechanism involving the central ruthenium atom, the macrocycle, and the $NO_2$ molecule.

## References and Notes

(1) Leznoff, C. C.; Lever, A. B. *Phthalocyanines. Properties and Applications*; VCH Publishers: Cambridge, U.K., 1989, 1993, and 1996; Vols. 1−4.

(2) Pagani, R. *Chem. Eng. News* **1996**, 22.

(3) Simon, J.; Andrè, J.-J. *Molecular Semiconductors*; Sprinter Verlag: Berlin, 1985.

(4) Snow, A. W.; Barger W. R. In *Phthalocyanines. Properties and Applications*; Leznoff, C. C., Lever, A. B., Eds.; VCH Pubblishers, (LSK) Ltd.: Cambridge, U.K., 1989; Vol. 1, p 341.

(5) Felici, R. *Rigaku J.* **1995**, *12*, 1.

(6) Caminiti, R.; Rossi Albertini, V. *Int. Rev Phys. Chem.* **1999**, *18* (2), 263.

(7) Parrat, L. G. *Phys. Rev.* **1954**, *95*, 359.

(8) Caminiti, R.; Sadun, C.; Rossi, V.; Cilloco, F.; Felici, R. Patent No. 01261484, Italy, 1993.

(9) Caminiti, R.; Carbone, M.; Panero, S.; Sadun, C. *J. Phys. Chem. B* **1999**, *103*, 47.

(10) Capobianchi, A.; Paoletti, A. M.; Pennesi, G.; Rossi, G.; Caminiti, R.; Ercolani, C. *Inorg. Chem.* **1994**, *33*, 4635.

(11) Caminiti, R.; Capobianchi, A.; Marovino, P.; Paoletti, A. M.; Pennesi, G.; Rossi, G. *Thin Solid Films* **2001**, *382*, 74.

(12) Generosi, R.; Miriametro, A. *Rev. Sci. Instrum.* **1982**, *53*, 9.

(13) Capobianchi, A.; Marovino, P.; Paoletti, A. M.; Pennesi, G.; Rossi, G. ICPP-1 (First Iternational Conference on Porphyrins and Phthalocyanines), Dijon, France, 25−30 June, 2000.

(14) Sinha; Sirota; Garoff; Stanley. *Phys. Rev. B* **1988**, *38*, 2297.

(15) Capobianchi, A.; Paoletti, A. M.; Pennesi, G.; Rossi, G. Unpublished results.